Dynamic and static correlation functions in the inhomogeneous-Hartree-Fock-state approach with random-phase-approximation fluctuations

J. Lorenzana*
International School for Advanced Studies, Via Beirut 4, 34014 Trieste, Italy

M. D. Grynberg† and L. Yu‡
International Center for Theoretical Physics, Strada Costiera 11, 34014 Trieste, Italy

K. Yonemitsu§ and A. R. Bishop
Theoretical Division, Los Alamos National Laboratory, Los Alamos, New Mexico 87545
(Received 13 July 1992)

The ground-state energy and static and dynamic correlation functions are investigated in the inhomogeneous-Hartree-Fock (IHF) plus random-phase-approximation (RPA) approach applied to a one-dimensional spinless-fermion model showing self-trapped doping states at the mean-field level. Results are compared with those obtained using homogeneous HF and exact diagonalization. RPA fluctuations added to the generally inhomogeneous-HF ground state allow the computation of dynamical correlation functions that compare well with exact diagonalization results. The RPA correction to the ground-state energy agrees well with the exact results at strong- and weak-coupling limits. We also compare it with a related quasiboson approach. The instability towards self-trapped behavior is signaled by a RPA mode with frequency approaching zero.

I. INTRODUCTION

Inhomogeneous mean-field states arise in many different contexts of many-body condensed-matter[1–11] and nuclear physics.[12] In particular, recently there has been considerable interest in the low-carrier-concentration regime of strongly correlated systems in connection with high-temperature superconductors.[5–8,13] Here we investigate the advantages and weaknesses of an inhomogeneous Hartree-Fock (IHF) approach plus random-phase-approximation (RPA) fluctuations. We use RPA to denote time-dependent Hartree Fock in the small amplitude oscillation limit as opposed to the usual meaning in condensed matter as a time-dependent Hartree approach.

We illustrate the method in a one-dimensional spinless-fermion model used in connection with modeling high-temperature superconductors,[7,13,14] and one-dimensional charge-transfer systems.[15] The model has the advantage for our propose that it supports nontrivial self-trapped states[7] at the mean-field level and is simple enough to allow exact diagonalization on relatively large chains.[16]

We first obtain homogeneous (HHF) and inhomogeneous Hartree-Fock solutions (Sec. III) and compute the ground-state energy (Sec. IV) as well as static correlation functions (Sec. V). These are compared with exact diagonalization results obtained with the Lanczos method.[17] The IHF approach gives better results for the ground-state energy and describes short-distance correlation functions better than its homogeneous counterpart. The range of validity of the approximation is discussed in Sec. II B.

In a second step, RPA fluctuations are added through the matrix form of RPA used in nuclear physics problems.[12] This allows us to compute dynamical correlation functions (Sec. VI) that compare well with exact diagonalization results reported in the literature.[14]

For both strong- and weak-coupling limits the correlation energy in RPA agrees quite well with the exact result. A related approach that amounts to treating the electron-hole pairs as bosons (quasiboson approximation) overestimates the correlation energy by a factor of 2 in weak coupling due to double counting.

The Hartree-Fock self-trapped solution appears above a critical value of the interaction. The transition is sharp at the mean-field level and is signaled by a RPA mode with frequency approaching zero. Above the transition the homogeneous Hartree-Fock solution has unstable RPA modes with imaginary frequencies.

II. INHOMOGENEOUS HARTREE-FOCK PLUS RPA APPROACH

A. Formalism

Here we sketch the formalism we are using. A more detailed discussion can be found in many nuclear physics textbooks.[12] We describe the RPA fluctuations in terms of a quasiboson approach because of its intuitive appeal. However, great care must be taken in interpreting the quasiboson expressions because of frequent double counting issues, as in one-body correlation functions[18,19] and the ground-state energy.[12] From now on we call the quasiboson (QB) approach the naive interpretation of the QB expressions, and RPA those results that can be derived

by solving a Bethe-Salpeter equation for the particle-hole Green function including ladder and bubble diagrams. The difference will become clear at the end of this subsection, where we exhibit different expressions for the correlation energy in these two approaches.

The Hamiltonian we consider is

$$H = \sum_l [(-1)^l \Delta c_l^\dagger c_l + t(c_l^\dagger c_{l+1} + \text{H.c.}) + G n_l n_{l+1}], \quad (1)$$

where $c_l^\dagger$ creates a spinless fermion on site l and $n_l = c_l^\dagger c_l$. We use units in which the hopping-matrix element $t = 1$. Δ describes the difference of the site energy for even and odd sites and G is the nearest-neighbor Coulomb repulsion. By means of Wick's theorem the original Hamiltonian [Eq. (1)] can be exactly rewritten as

$$H = E_{\text{HF}} + : H_{\text{HF}} : + G \sum_l : n_l n_{l+1} : . \quad (2)$$

The HF Hamiltonian is then given by

$$H_{\text{HF}} = \sum_l (\tilde{E}_l c_l^\dagger c_l + \tilde{t}_l c_l^\dagger c_{l+1} + \tilde{t}_l^* c_{l+1}^\dagger c_l) , \quad (3)$$

where

$$\tilde{E}_l = (-1)^l \Delta + G(\langle n_{l+1} \rangle + \langle n_{l-1} \rangle) ,$$
$$\tilde{t}_l = t + G \langle c_l c_{l+1}^\dagger \rangle . \quad (4)$$

Here ":" denotes normal product and "$\langle\,\rangle$" expectation value in the HF vacuum:

$$|\text{HF}\rangle = \prod_{\nu<F} a_\nu^\dagger |0\rangle . \quad (5)$$

The Hartree-Fock energy is $E_{\text{HF}} = \langle H \rangle$.

The operators $a_\nu^\dagger$ are obtained through a canonical transformation that diagonalizes H_{HF},

$$a_\nu^\dagger = \sum_l \psi_{\nu l} c_l^\dagger . \quad (6)$$

The last term in Eq. (2) represents the residual interaction between the particles (V_{res}) . The main effect of V_{res} is to create electron-hole excitations over $|\text{HF}\rangle$ and to produce scattering among them. The effect of : H_{HF} : is to limit the electron-hole pair production, because of the energy cost $\epsilon_m - \epsilon_i$. Here ϵ_μ are the single-particle HF energies and we use m, n to label states above the Fermi level F; i, j for states below and μ, ν, σ, ρ in general. After normal ordering the residual interaction shows a number of terms representing different scattering processes, as well as particle-hole production and annihilation. Now, assuming that the number of particles above F (or equivalently holes below F) will be small in the true ground state we keep only those terms in the residual interaction that represent creation or destruction of particle hole pairs, or scattering among themselves. We expect the above condition to be satisfied if we start from a "good" HF state, even in strong coupling. Identifying sufficiently good states requires searching for the lower-energy, truly relaxed mean-field states.

We would like to find a correlated vacuum $|\text{RPA}\rangle$ and a set of operators Q_λ that diagonalize the Hamiltonian in this subspace. However, even with the above simplifications this cannot be done exactly.

We define the particle-hole creation operators,

$$b_{mi}^\dagger = a_m^\dagger a_i , \quad (7)$$

and their Hermitian conjugates b_{mi}. The next approximation is to treat $b_{mi}^\dagger$ and b_{mi} as boson creation and destruction operators. Boson commutation relations are obtained if one takes the expectation value of the commutators in the $|\text{HF}\rangle$ state. The fact that one uses the HF vacuum and not the new vacuum $|\text{RPA}\rangle$ implies an internal inconsistency of the QB approximation.[18] This is not a big problem if, as expected, $|\text{RPA}\rangle$ is not too far from $|\text{HF}\rangle$. Now we proceed to construct a boson Hamiltonian (H_{QB}) in such a way that, with the above approximations, it reproduces the commutation relations of the original Hamiltonian. The result is

$$H_{\text{QB}} = E_{\text{HF}} + \quad (8)$$
$$\sum_{mi,nj} (A_{mi,nj} b_{mi}^\dagger b_{nj} + \tfrac{1}{2} B_{mi,nj} b_{mi}^\dagger b_{nj}^\dagger + \tfrac{1}{2} B_{mi,nj}^* b_{nj} b_{mi}),$$

where the RPA matrices[12] are given by

$$A_{mi,nj} = (\epsilon_m - \epsilon_i)\delta_{mn}\delta_{ji} + \langle jm|V|ni\rangle - \langle jm|V|in\rangle ,$$
$$B_{mi,nj} = \langle mn|V|ij\rangle - \langle mn|V|ji\rangle . \quad (9)$$

In our case the matrix elements of the interaction are

$$\langle \mu\nu|V|\sigma\rho\rangle$$
$$= \sum_l G(\psi_{\mu l}^* \psi_{\nu l+1}^* \psi_{\rho l+1} \psi_{\sigma l} + \psi_{\mu l}^* \psi_{\nu l-1}^* \psi_{\rho l-1} \psi_{\sigma l}) . \quad (10)$$

The constant term in Eq. (8) can be obtained by taking the expectation value of H_{QB} in the $|\text{HF}\rangle$ state and using the fact that it is the vacuum of the b_{mi} operators.

H_{QB} is diagonalized by the following Bogoliubov transformation:

$$Q_\lambda^\dagger = \sum_{mi} (X_{mi}^\lambda b_{mi}^\dagger - Y_{mi}^\lambda b_{mi}) . \quad (11)$$

$Q_\lambda^\dagger$ creates an excitation of frequency $\omega_\lambda > 0$ over the new vacuum $|\text{RPA}\rangle$ and its Hermitian conjugate destroys it. $\lambda > 0$ ($\lambda < 0$) labels amplitudes and frequencies related to creation (destruction) operators. X^λ, Y^λ, and ω_λ are obtained from the RPA eigenvalue problem:

$$\begin{pmatrix} A & B \\ B^* & A^* \end{pmatrix} \begin{pmatrix} X^\lambda \\ Y^\lambda \end{pmatrix} = \omega_\lambda \begin{pmatrix} X^\lambda \\ -Y^\lambda \end{pmatrix} . \quad (12)$$

Positive (negative) eigenvalues correspond to creation (destruction) operators in Eq. (11) and obey the normalization condition:

$$(X^{\lambda\dagger},\ Y^{\lambda\dagger}) \begin{pmatrix} X^{\lambda'} \\ -Y^{\lambda'} \end{pmatrix} = \delta_{\lambda,\lambda'} \text{sgn}(\omega_\lambda) . \quad (13)$$

With this transformation the Hamiltonian can be put in the canonical form:

$$H_{\mathrm{QB}} = E_{\mathrm{HF}} + E_{\mathrm{QB}} + \sum_{\lambda>0} \omega_\lambda Q_\lambda^\dagger Q_\lambda. \tag{14}$$

Matrix elements of operators can be calculated using the relations,

$$\langle \mathrm{RPA}|b_{mi}|\lambda\rangle = X_{mi}^\lambda$$
$$\langle \mathrm{RPA}|b_{mi}^\dagger|\lambda\rangle = Y_{mi}^\lambda, \tag{15}$$

with $|\lambda\rangle = Q_\lambda^\dagger|\mathrm{RPA}\rangle$.

The constant term can be obtained as before by taking the expectation value in the $|\mathrm{HF}\rangle$ state and is given by[12]

$$E_{\mathrm{QB}} = \tfrac{1}{2}\left(\sum_\lambda \omega_\lambda - \mathrm{Tr}A\right). \tag{16}$$

Unfortunately, Eq. (16) is not the same expression that one would obtain diagrammatically for the RPA correction to the Hartree-Fock ground-state energy. The problem is that, as compared with diagrammatic expansions, the above expression double-counts the second-order term[12] in the residual interaction. We believe the problem is related to the internal inconsistency of the QB approximation mentioned above and should be cured in a fully self-consistent[18,20] approach. The correct RPA expression is obtained by subtracting the overcounted part:

$$E_{\mathrm{RPA}} = E_{\mathrm{QB}} - \left(-\frac{1}{4}\sum_{mi,nj} \frac{|\langle ij|V|mn\rangle|^2}{\epsilon_m + \epsilon_n - \epsilon_i - \epsilon_j}\right). \tag{17}$$

Note that the subtracted perturbation in the above expression is not due to the bare interaction but the residual interaction, which is small whenever the true ground state is close to the HF state. For example, for the $t \to 0$ limit the Hamiltonian is diagonal in real space; the eigenstates can be written as Slater determinants and the off-diagonal matrix elements of the interaction, like the ones appearing in Eq. (17), vanish.

Note also that the eigenvalue problem is the same as that obtained with diagrammatic techniques. In this sense the two approximations are equivalent to each other.

B. Range of validity of the approximations

As discussed above, the RPA is good if the number of electron-hole excitations over the mean-field state is small. In principle this can be true even in the strong-coupling limit provided the ground state is close to a Slater determinant. This approximation breaks down in regions of parameter space very close to phase changes in the mean-field state. Generally, in the vicinity of such pseudophase transitions the system is very anharmonic and the fluctuations are too large.

At the present level of approximation another constraint arises from the lack of translational motion. One is neglecting the fact that the self-trapped state (which we will call a "polaron," in analogy with self-trapping in the presence of electron-phonon interaction) will tunnel from a given localized state after some time τ. This means that one expects the approximation to be valid for short times ($t < \tau$), large energies and frequencies ($\omega > 1/\tau$), and short wavelengths ($l < c\tau$ with c as some characteristic velocity of the order of the Fermi velocity). Note that $1/\tau$ is of the order of the polaron bandwidth. Its estimation is beyond the present approximation.

III. HARTREE-FOCK AND RPA STATES

At half-filling the charge distribution is uniform and the mean-field equations can be solved in reciprocal space. There are two bands separated by a gap and the chemical potential is in the middle of the gap. The effect of G, Eq. (4) is to increase the gap and to renormalize the bandwidth.

As mentioned in the Introduction, when one particle is added to the system, it generally self-traps[7] at the HF level and forms a polaronlike state. In Fig. 1 we show the HF charge distribution for different values of G for a chain of $N = 10$ unit cells. The polaron is small for large G. As G decreases it extends more and more, up to a critical value of the interaction ($G_c = 1.58$ for $\Delta = 0.3$) when it reaches the size of the box [Fig. 1(b)]. At this point the HF ground state changes and it becomes homogeneous [Fig. 1(a)]. Below this value the HF state is translationally invariant. This "phase transition" is an artifact of the HF approximation. No sharp transition occurs in the exact results and one has to think in terms of a smooth, although possibly rapid, crossover. At the RPA level the transition is signaled by the softening of the corresponding modes (Fig. 2). On the uniform side, the modes can be labeled by the momentum q transferred in the scattering process. Except for the modes with $q = 0, \pi$, all the other modes are doubly degenerate due to the symmetry $q \to -q$.

The normal modes around the mean-field state are characterized by the so-called transition densities $\langle RPA|n_l|\lambda\rangle$. They determine the dynamic components of the expectation value of n_l in a wave packet formed by the ground state and small admixtures of excited states: viz.,

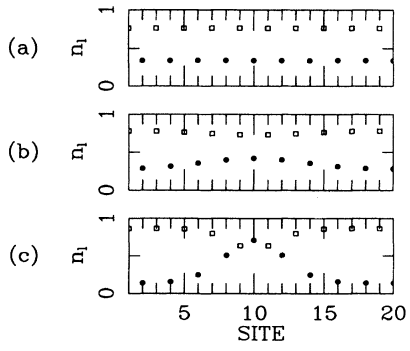

FIG. 1. Site occupation for one particle added to the half-filling case (a) $N = 10$, $\Delta = 0.3$, $G = G_c - \eta$; (b) $G = G_c + \eta$; and (c) $G = 2.5$. η is a small number for which the equations can be solved without convergence problems. Solid circles correspond to the even sites and squares correspond to the odd sites.

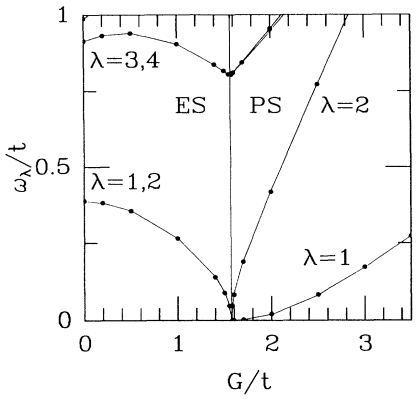

FIG. 2. Lowest RPA frequencies as a function of the interaction G for one particle added to half-filling, $N = 10$ and $\Delta = 0.3$. The vertical line indicates the transition between the extended state (ES) and polaron state (PS).

$$
\begin{aligned}
&|\Psi(t)\rangle = |\mathrm{RPA}\rangle + \sum_{\lambda>0} c_\lambda e^{-i\omega_\lambda t}|\lambda\rangle, \\
&\langle\Psi(t)|n_l|\Psi(t)\rangle = n_l^0 + \delta n_l(t), \\
&n_l^o = \langle \mathrm{RPA}|n_l|\mathrm{RPA}\rangle, \\
&\delta n_l(t) = \sum_{\lambda>0} c_\lambda \langle \mathrm{RPA}|n_l|\lambda\rangle e^{-i\omega_\lambda t} + \mathrm{H.c.} + O(c_\lambda^2).
\end{aligned}
\tag{18}
$$

Similar expressions can be written for the off-diagonal elements of the one-body density matrix. In general, they are computed by expressing the one-body operators in terms of the particle-hole operators, through Eq. (7), and using the relations of Eq. (15). In our case, the transition densities can be taken as real. Note that in the last expression of Eq. (18) the vanishing of a frequency means the conversion of a dynamic distortion of the density into a static distortion. In Fig. 3(a) we show the transition density for the mode that goes to zero frequency. The distortion is of the charge-transfer (CT) type at short distances, i.e., the charge increases on even atoms and decreases on odd atoms, or vice versa, in a time-dependent wave packet as discussed above. At long distances the charge flows from one half of the chain to the other, preempting the polaron effect. Due to the fact that even states have more weight in the upper band which is partially filled, the amplitude is larger at those sites indicating more probability for the charge to flow. Comparison with Figs. 1(a) and 1(b) makes evident the "freezing" of this dynamical fluctuation.

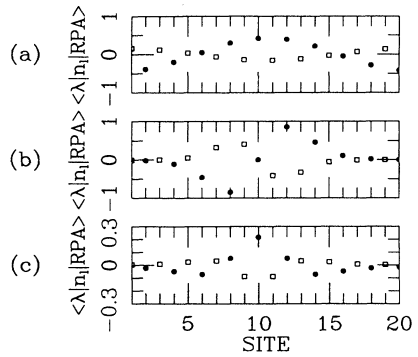

FIG. 3. Transition densities for one particle added to the half-filling case, $N = 10$, $\Delta = 0.3$, and different values of G. (a) $\lambda = 1$, $G = G_c - \eta$. η is a small number with which the equations can be solved without convergence problems. The $\lambda = 2$ case is similar but with nodes on sites where the $\lambda = 1$ case shows maxima. (b) $G = 2.5$ and $\lambda = 1$ (oscillation in the pinning potential). (c) $G = 2.5$, $\lambda = 2$ (amplitude mode). Solid circles correspond to the even sites and squares correspond to the odd sites.

Above the transition the inhomogeneous mean-field state breaks the translational symmetry of the lattice. If this were a continuous symmetry the Goldston theorem would guarantee the existence of a zero-energy mode related to the translational motion of the polaron that restores the symmetry. Here, because of the discrete character of the broken symmetry, the polaron is pinned to the lattice and at this level of approximation there is no translational motion but oscillation in the pinning potential. So this mode [Fig. 3(b)] has a finite frequency except right at the transition. Real translational motion can be thought of as tunneling between different pinning centers.

Below the transition the lower-energy modes are collective. Their frequencies are separated appreciably from the Hartree-Fock single-particle excitations. Above the transition they become localized whereas the high-energy modes remain extended and have a single particle-hole character.

It is interesting to follow how the modes change at the transition. The two degenerate CT modes split. One becomes the translational mode [Fig. 3 (b)], the other conserves its shape but localizes and becomes an amplitude mode [Fig. 3 (c)]. When the transition is approached from above, both modes become soft.

IV. GROUND-STATE ENERGY

Here we compare the result of the different approximations for the ground-state energy with exact diagonalization results performed in systems of the same size and the same boundary conditions. We compute the correlation energy $E_c^{N+i} = E^{N+i} - E_{\mathrm{HF}}^{N+i}$. E^{N+i} is the ground-state energy for the system with $N+i$ particles. For E_{HF}^{N+i} we take the lowest (generally inhomogeneous) HF state.

At half-filling the HF ground state is homogeneous and the HF energy reproduces correctly the behavior of the ground-state energy as a function of G and slightly underestimates it due to the variational nature. In Fig. 4 we show the exact correlation energy per site as a function of G and compare it with the QB and RPA results. In the small coupling regime RPA gives the correct quadratic behavior as a function of G, whereas QB overshoots it by a factor of 2, as explained in the previous section.

Away from half-filling the behavior is different depending on how we approach the strong-coupling limit. If $G/t \to \infty$ and Δ is kept zero the added particle separates into a kink-antikink soliton[21,7] pair. If Δ is small, the solitons are weakly bound (in a small ring the ef-

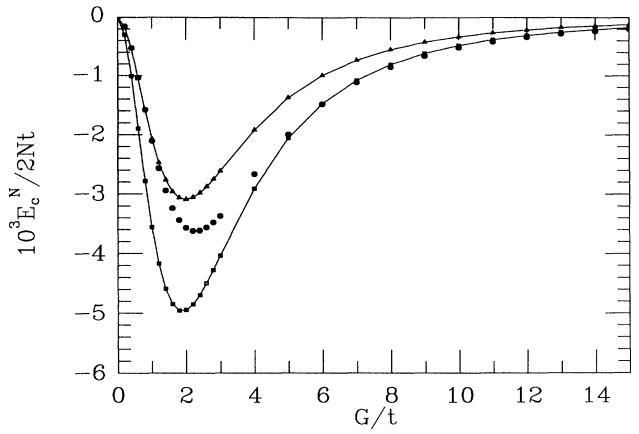

FIG. 4. Correlation energy per site as a function of the interaction G for $N = 10$ and $\Delta = 0.5$. Solid circles are the exact results, squares correspond to the QB, and triangles correspond to the RPA.

fect can be negligible) and they can move with an effective bandwidth of the order t. This band motion of solitons is not included in our approach making the correlation energy in modulus underestimated with respect to the true value. On the other hand, in the limit $G/t, \Delta/t \to \infty$, keeping Δ/G constant, the kink and antikink are tightly bound and the ground state is a polaron whose bandwidth goes to zero. We illustrate this behavior by showing the correlation energy required to add a polaron ($E_p^c = E_c^{N+1} - E_c^N$) (Fig. 5). As G increases the fact that one neglects the band motion of the polaron become less and less important and hence E_p^c calculated in RPA converges to the exact result. On the other hand, when G goes to zero the particle is not any more self-trapped and again one gets good agreement with the exact result. Close to G_c other anharmonic effects become important. We note that the homogeneous solutions for $G > G_c$ always have higher energy than the corresponding inhomogeneous ones. Moreover, since the RPA spectra have imaginary frequencies, a correction to the HHF energy does not make sense.

V. STATIC CORRELATION FUNCTIONS

Here we compare static correlation function calculated in the IHF and HHF with exact diagonalization results obtained with the Lanczos method.[17] Because the HF solution breaks the translational invariance the static correlation functions depend not only on the distance to the origin, but also on the position of the origin itself. We denote by $|\mathrm{HF}, r_o\rangle$ the HF state centered at r_o. There are N nonorthogonal HF wave functions with the same energy characterized by the position r_o of the center of the polaron state. The next level of approximation would be to compute matrix elements of the Hamiltonian between the different IHF states and to construct Bloch states. A simpler approach is to completely neglect the overlap and to consider the different HF solutions as orthogonal degenerate states. Then, for example, the one-body density matrix can be calculated as a $T = 0$ thermodynamic average, that is

$$[\langle c_{r_o}^\dagger c_r \rangle] = \frac{1}{N} \sum_{s=0}^{N-1} \langle c_{r_o+2s}^\dagger c_{r+2s} \rangle. \tag{19}$$

In Fig. 6 we show the off-diagonal part of the one-body density matrix for a single particle added to the system and as a function of the distance from the origin at an even site, for $\Delta = 0.5$ and $G = 3$. The Fourier transform of such a quantity gives the momentum distribution function and the long-distance behavior is related to the Fermi-level discontinuity Z. For the IHF state it decays exponentially, indicating a fictitious insulating behavior ($Z = 0$). Such a long-distance failure is beyond the range of applicability of the present calculation and should be cured in a polaron band approach as explained above. On the other hand, the HHF gives a better long-distance behavior but, as expected, overestimates the Z. At short

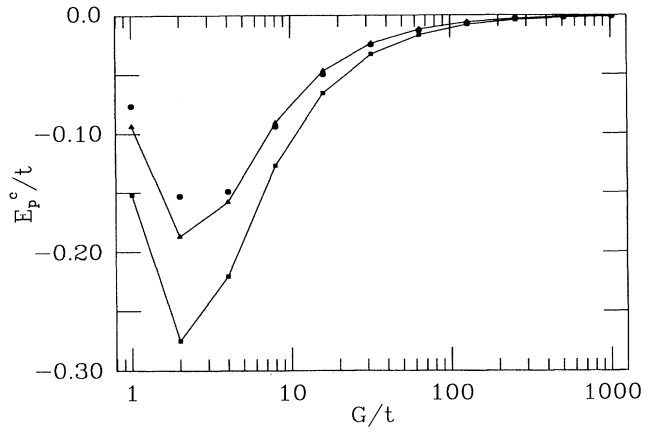

FIG. 5. Correlation energy of a polaron as a function of the interaction G keeping $G/\Delta = 2$ for $N = 10$. Solid circles are the exact results, squares correspond to the QB, and triangles correspond to the RPA.

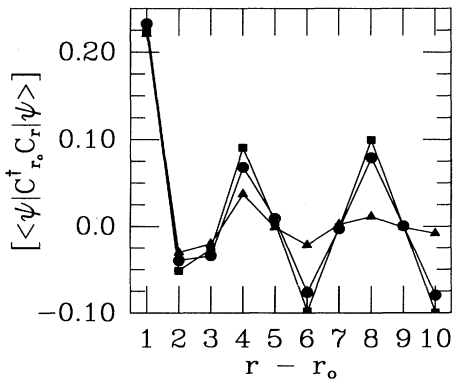

FIG. 6. Off-diagonal part of the density matrix as a function of distance for one particle added to the half-filling case, $N = 10$, $\Delta = 0.5$, $G = 3$. r_o corresponds to an even site. Solid circles are the exact results, squares correspond to the HHF, and triangles correspond to the IHF.

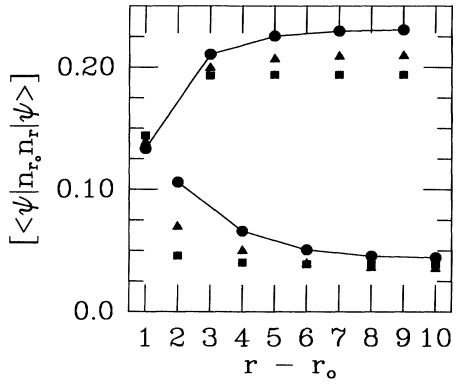

FIG. 7. Charge-charge correlation function as a function of distance for one particle added to the half-filling case, $N = 10$, $\Delta = 0.5$, $G = 3$. Solid circles are the exact results, squares correspond to the HHF, and triangles correspond to the IHF.

distance this quantity shows only slight differences between the two approaches as one would expect because the important correlations are due to local distortions of charge densities around the added particle. This is illustrated in the two-body correlation function that we plot in Fig. 7. We see that IHF does better than its homogeneous counterpart at short distance, and, unexpectedly, at long distance as well. Importantly, at short distances it takes into account the local distortion of the charge better than HHF.

VI. DYNAMIC CORRELATION FUNCTIONS

From the RPA eigenvectors it is easy to compute dynamical correlation functions of the form

$$C_{AB}(t-t') = \langle \mathrm{RPA}|A(t)B(t')|\mathrm{RPA}\rangle, \tag{20}$$

where A and B are one-body operators. In fact the imaginary part of the Fourier transform admits the following

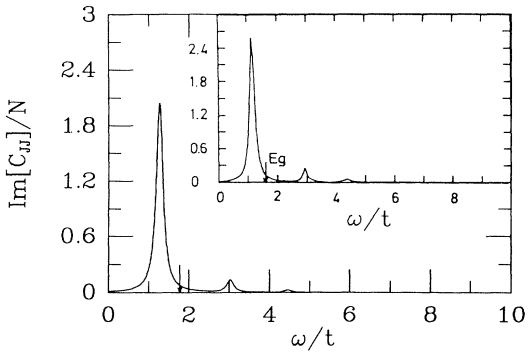

FIG. 8. Imaginary part of the current-current correlation function in the RPA. We add a small imaginary part to the energy ($\eta = 0.1$) in order to broaden the δ functions. $N = 8$, $\Delta = 0.25$, $G = 1$. The arrow indicates the value of the uniform HF gap. The inset shows the exact results of Ref. 16 and the arrow indicates the value of the gap in the single-particle spectral function.

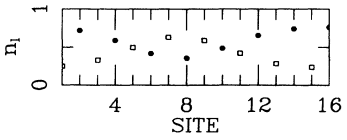

FIG. 9. Site occupation for the exciton state. $N = 8$, $\Delta = 0.25$, $G = 1$. Solid circles correspond to the even sites and squares correspond to the odd sites.

spectral representation:

$$\mathrm{Im}[C_{AB}(\omega)] = \sum_{\lambda>0}\langle \mathrm{RPA}|A|\lambda\rangle\langle\lambda|B|\mathrm{RPA}\rangle\delta(\omega-\omega_\lambda), \tag{21}$$

The matrix elements in Eq. (21) are given by the transition densities of Sec. III.

At the RPA level there are single-particle-hole excitations which have almost the same energy as the corresponding Hartree-Fock particle-hole excitations and collective excitations. At half-filling one expects the correlation between particles and holes to produce an excitonic peak below the lowest HF particle-hole excitation which corresponds to the mean-field gap. Such collective excitation can be seen in the current-current correlation function that gives the optical excitation spectra—in this case we use in Eq. (20) $A^\dagger = B = J$, where $J = -it\sum_l (c_l^\dagger c_{l+1} - c_{l+1}^\dagger c_l)$.

In Fig. 8 we show the imaginary part of the current-current correlation function for $N = 8$, $\Delta = 0.25$, $G = 1$, and antiperiodic boundary conditions. The arrow indicates the position of the Hartree-Fock gap. The result compares very well with the exact solutions of Ref. 16. In particular, the position of the excitonic peak below the gap is very close to the exact value. This pole gives the energy to create an exciton over the uniform state. The same excited state can be obtained in a rather different way. We can look for a site-dependent mean-field solution in which the lowest state of the upper band is full and the highest state of the lower band is empty.[7] Figure 9 shows such an example. The energy difference $\epsilon_e = E^N_{\mathrm{exciton}} - E^N$ gives the excitation energy in this approach and an interesting question is how it compares with the energy of the excitonic peak described above. In Fig. 10 we show the exciton creation energy for different values of Δ in the site-dependent HF and compare it with the RPA results and the exact diagonalization results of Ref. 14. The pentagons indicate the value of the uniform Hartree-Fock gap. The agreement is quite good. One should keep in mind that the RPA is a linearized theory, in this case around the uniform mean-field state. The above agreement suggests that the estimate of Fig. 9 is not too far from a linear excitation around the uniform state. Note however that the energy is not very sensitive to small errors due to nonlinearities in the wave function.

VII. CONCLUSIONS

We have calculated the ground-state energies, static and dynamic correlation functions in the IHF + RPA

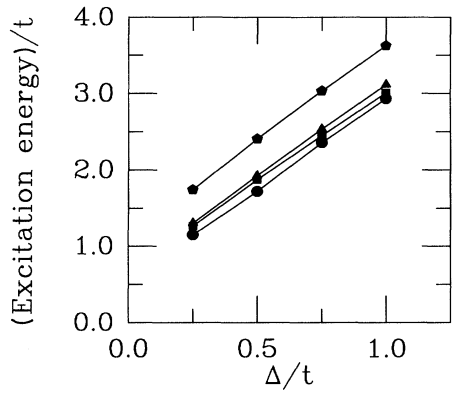

FIG. 10. Excitation energy to create an exciton as a function of Δ. Solid circles are the exact results, squares correspond to the RPA, and triangles correspond to the IHF. For comparison we also plot the uniform Hartree-Fock gap (pentagons).

approach for a simple spinless-fermion model.

We showed how the transition between polaronic behavior and band motion is signaled at the RPA level by collective modes that become soft. A similar effect in a very complex system[11] explains anomalous behavior of optical and other properties of high-temperature superconductors.

The calculations were compared with exact diagonalization results. We showed that IHF describes short-range correlations better in this strongly correlated model than the HHF. However, due to the fact that the first approach breaks translational invariance, all properties related to the metallic behavior are not properly described at this level of approximation. This is not unexpected because the metallic regime is a long-distance behavior and hence it is out of the range of validity of the present level of approximation. In this sense this approach is complementary to other techniques like bosonization[22] or renormalization group that are expected to work in the opposite limit (long wavelength and low energies). A possible extension of the method would be to form polaron bands. In principle, this should give better long-distance properties but requires additional approximations. One appealing method to calculate matrix elements between different HF minima, would be to perform an instanton calculation. This would require an imaginary time-dependent HF calculation which is beyond the present work.

Another advantage of working with the stable IHF solutions instead of the HHF ones is that one can easily perform the matrix RPA on the basis of the IHF solutions and obtain the linear-excitation spectra of the system. It allows computation of dynamical correlation functions that compare well with the exact ones. It can be performed in larger systems and faster than exact diagonalization methods but also, by plotting the site-dependent IHF densities and RPA transition densities, one can visualize the physics involved.

It is interesting to note that the energy to create an exciton is very close to the exact one in both the RPA and in a site-dependent approach in which the occupations of the IHF orbitals are constrained to produce the excited state.

Finally we note that the technique is flexible enough to study different competing interactions.[8,9] In this sense we expect that it will provide a good understanding of strong correlations in realistic models.

ACKNOWLEDGMENT

The work at Los Alamos was supported by the USDOE.

*Present address: Laboratory of Applied and Solid State Physics, University of Groningen, Nijenborgh 4, 9747 AG Groningen, The Netherlands.
†Present address: Department of Theoretical Physics, University of Oxford, 1 Keble Road, Oxford OX1 3NP, U.K.
‡Permanent address: Institute of Theoretical Physics, Chinese Academy of Sciences, Beijing 100080, China.
§Present address: International Center for Theoretical Physics, Strada Costiera 11, 34014 Trieste, Italy.

[1]A. Auerbach and B. L. Larson, Phys. Rev. Lett. **66**, 2262 (1991).
[2]J.A. Vergés, E. Louis, P.S. Lomdahl, F. Guinea, and A.R. Bishop, Phys. Rev. B **43**, 6099 (1991).
[3]A.R. Bishop, P.S. Lomdahl, J.R. Schrieffer, and S.A Trugman, Phys. Rev. Lett. **61**, 2709 (1988).
[4]I. Batistić and A.R. Bishop, Phys. Rev. B **45**, 5282 (1992).
[5]J. Zaanen and O. Gunnarsson, Phys. Rev. B **40**, 7391 (1989).
[6]Z.B. Su, Y.M. Li, W.Y. Lai, and L. Yu, Phys. Rev. Lett. **63**, 1318 (1989).
[7]J. Lorenzana and L. Yu, Phys. Rev. B **43**, 11 474 (1991).
[8]K. Yonemitsu, I. Batistić, and A.R. Bishop, Phys. Rev. B **44**, 2652 (1991).
[9]K. Yonemitsu, A.R. Bishop, and J. Lorenzana, Phys. Rev. Lett. **69**, 965 (1992).
[10]K. Yonemitsu and A.R. Bishop, Phys. Rev. B **45**, 5530 (1992).
[11]J. Lorenzana and L. Yu, Phys. Rev. Lett. **70**, 861 (1993).
[12]J.-P. Blaizot and G. Ripka, *Quantum Theory of Finite Systems* (MIT, Cambridge, Massachusetts, 1986).
[13]V. J. Emery, Phys. Rev. Lett. **65**, 1076 (1990).
[14]C. A. Balseiro, A.G. Rojo, E.R. Gagliano, and B. Alascio, Phys. Rev. B **38**, 9315 (1988).
[15]R. Bruinsma, P. Bak, and J.B. Torrance, Phys. Rev. B **27**, 456 (1983).
[16]E.R. Gagliano and C.A. Balseiro, Phys. Rev. B **38**, 11 766 (1988).
[17]E. Dagotto and A. Moreo, Phys. Rev. D **31**, 865 (1985).

[18]D.J. Rowe, Phys. Rev. **175**, 1283 (1968).
[19]R.E. Johnson, R.M. Dreizler, and A. Klein, Phys. Rev. **186**, 1289 (1969).
[20]N. Meshkov, A.J. Glick, and H.J. Lipkin, Nucl. Phys. **62**, 199 (1965).
[21]J. Hubbard, Phys. Rev. B **17**, 494 (1978).
[22]V.J. Emery, in *Highly Conducting One-Dimensional Solids*, edited by J.T. De Vreese, R.P. Evrard, and V.E. Van Doren (Plenum, New York, 1987).